

Supporting Information for

Novel Positive Allosteric Modulators of the Human $\alpha 7$ Nicotinic Acetylcholine Receptor[†]

Hugo R. Arias[‡], Ruo-Xu Gu^{§,□}, Dominik Feuerbach^{||}, Bao-Bao Guo[#],

Yong Ye[#], and Dong-Qing Wei^{§,*}

[§] Luc Montagnier BioMedical Research Institute (LMBMRI) and National Key Lab. Of Microbial Metabolism, College of Life Sciences and Biotechnology, Shanghai Jiaotong University, Shanghai, China

[‡] Department of Pharmaceutical Sciences, College of Pharmacy,
Midwestern University, Glendale, Arizona, USA

^{||} Neuroscience Research, Novartis Institutes for Biomedical Research, Basel, Switzerland

[#] Laboratory of Chemical Biology, Department of Chemistry, Zhengzhou University,
Zhengzhou, Henan, China

^{‡,□} Both co-authors are considered first authors of this work.

^{*} To whom correspondence should be addressed: Luc Montagnier BioMedical Research Institute (LMBMRI) and National Key Lab. Of Microbial Metabolism, College of Life Sciences and Biotechnology, Shanghai Jiao Tong University, 800 Dongchuan Road, Shanghai 200240, China. Telephone: 86-21-3420-4573. Fax: 86-21-3420-4573. E-mail: dqwei@sjtu.edu.cn.

Method

To give insight into the interaction between PAMs and the agonist/competitive antagonist site at different AChR interfaces, compound 2 (representative of compounds with PAM activity) was docked to the agonist site at the $\alpha 7/\alpha 7$, $\alpha 3/\beta 4$ and $\alpha 4/\beta 2$ interfaces, respectively. Then, 1-ns molecular dynamics simulations were performed to investigate the stability of the complexes. For comparison, (+)-epibatidine was docked to the agonist site at the $\alpha 7/\alpha 7$ interface and molecular simulations were also conducted. To shorten the time used in the searching of the molecular conformations, simulations were performed at high temperature (450K). Since we only want to observe the stability of the ligands, the Ca atoms were constrained to preserve the 3D structure of the protein.

Results

PAMs do not Bind to the AChR Agonist Sites. The dynamics simulation results show that (+)-epibatidine binds to the $\alpha 7/\alpha 7$ interface in a steady manner, whereas compound 2 moves away from its initial position at the $\alpha 7/\alpha 7$, $\alpha 3/\beta 4$ and $\alpha 4/\beta 2$ agonist sites (Figs. S1B-E). The larger RMSD values of compound 2 at the different agonist sites (~0.4-0.8 nm) compared to that for (+)-epibatidine (~0.2 nm) at the $\alpha 7/\alpha 7$ interface (Fig. S1A) also indicate that these PAMs are unstable when binding to the agonist sites.

Hydrogen Bonds are important for PAM Activity. More hydrogen bonds are found in the $\alpha 7$ AChR-compound 2 complex (Fig. S2A) than that found in the complex between the $\alpha 3\beta 4$ or $\alpha 4\beta 2$ AChR and compound 2 (Figs. S2B,C). Two hydrogen bonds are formed in the $\alpha 7$ -PAM complex, one between the oxygen atom from the carboxyl group of compounds 2-4 and the Asn104 side chain at the (-) face and the other between the nitrogen of the compound's amide group and the Lys84 backbone at the (+) face (Fig. S2A). In the $\alpha 3\beta 4$ -ligand complex, however, the nitrogen atom forms a hydrogen bond with the side chain of the homologous residue Trp83 at the (+) face, whereas there is no hydrogen bond with the (-) face (Fig. S2B). In the case of the $\alpha 4\beta 2$ AChR, the determined distances between the oxygen atom

of the amide linkage and the backbone oxygen and the side chain nitrogen of the homologous residue Arg84 at the (+) face are both in the range of forming hydrogen bonds, whereas hydrogen bonds with the (-) face are not found (Fig. S2C).

To compare the hydrogen bond interactions of compounds 2-4 with that of compound 1 at the $\alpha 7/\alpha 7$ interface, the distances between the hydrogen bond donors and acceptors were calculated. The distance for each hydrogen bond for compounds 2-4 is ~ 3.30 Å and ~ 2.80 Å, respectively, whereas these distances are longer for compound 1 (compare Figs. S2A,D). The docking results of compound 1 show that although the benzene ring is aligned with that of compounds 2-4 (compare Figs. S2A,D), its amide group is shifted away from this alignment because of steric hindrance mediated by the methyl group located between the amide and benzene groups (Fig. 1). As a result of this structural shifting, the distance between the nitrogen of the amide group and the Asn104 side chain is augmented to 6.33 Å whereas that between the oxygen of the carboxyl group and the Lys84 side chain is enlarged to 3.08 Å (Fig. S2D). Hence, although compound 1 is structurally similar to compounds 2-4 (see Fig. 1), the hydrogen bond interaction between the amide group and Asn104 that are important for the PAM activity elicited by compounds 2-4 is very improbable to take place by compound 1. However, compound 1 may still form a hydrogen bond with the (+) face.

The PAM site in the $\alpha 7$ AChR is larger than that in the $\alpha 3\beta 4/\alpha 4\beta 2$ AChRs. In the $\alpha 7$ AChR, the furan ring of compounds 2-4 is positioned between the side chains from His102 and Lys84 (Fig. S2A). However, in $\alpha 3\beta 4/\alpha 4\beta 2$ AChRs, $\alpha 7$ -His102 is mutated to $\beta 2/\beta 4$ -Tyr104. Since Tyr104 has a larger side chain compared to that for His102, the space between Tyr104 and Lys84/Arg84 in the $\alpha 3/\beta 4$ and $\alpha 4/\beta 2$ interfaces is smaller (compare Figs. S2A-C). Supporting this structural difference, the calculated distance between the mass centers of the $\alpha 7$ -His102 and $\alpha 7$ -Lys84 side chains is 9.27 Å, whereas the distance between the $\alpha 4$ -Arg84/ $\alpha 3$ -Lys84 and the respective $\beta 2$ -Tyr104/ $\beta 4$ -Tyr104 side chains are 8.09 Å and 6.28 Å, respectively. The smaller volume in the $\alpha 3\beta 4/\alpha 4\beta 2$ AChR binding pockets precludes

the fitting of the furan ring in this domain, and consequently, these compounds cannot produce any PAM activity on these AChRs.

The postulated PAM sites at the $\alpha 7$ AChRs are not probable at the $\alpha 3\beta 4$ and $\alpha 4\beta 2$ AChRs.

Compound 2 was first docked to the three potential domains for PAMs: (1) the extracellular domain of the $\alpha 3/\beta 4$ (or $\alpha 4/\beta 2$) subunit interface, (2) the extracellular-transmembrane junction of $\alpha 3$ (or $\alpha 4$) subunit and (3) the transmembrane domain of the $\alpha 3$ (or $\alpha 4$) subunit. After docking compound 2 to the three potential PAM sites at the $\alpha 3\beta 4$ and $\alpha 4\beta 2$ AChRs, 10-ns molecular dynamics simulations were performed on the ligand-receptor complexes to evaluate their stability. The calculated RMSD values at the $\alpha 3/\beta 4$ interface and at the extracellular-transmembrane junction of the $\alpha 3$ subunit are ~0.4-0.5 nm, whereas that at the $\alpha 3$ transmembrane domain is about 0.6 nm (Fig. S3). The RMSD values for the PAM sites on the $\alpha 4\beta 2$ AChR are ~0.4-0.8 nm (Fig. S4). These values indicate that compound 2 is unstable when it binds to each one of these potential PAM sites on the $\alpha 3\beta 4$ and $\alpha 4\beta 2$ AChRs.

FIGURE S1: Molecular dynamics simulations of compound 2 at the agonist/competitive antagonist site on different AChR subunit interfaces and of (+)-epibatidine at the $\alpha 7/\alpha 7$ interface. (A) RMSD values for compound 2 bound to the agonist/competitive antagonist site at the $\alpha 7/\alpha 7$ (red line), $\alpha 3\beta 4$ (blue line), and $\alpha 4\beta 2$ (green line) interfaces, and for (+)-epibatidine bound to the $\alpha 7/\alpha 7$ interface (black line). Location of (B) (+)-epibatidine and (C) compound 2 before (blue) and after (green) 1-ns dynamics simulations at the $\alpha 7/\alpha 7$ interface, and of compound 2 at the (D) $\alpha 3\beta 4$ and (E) $\alpha 4\beta 2$ interfaces, respectively. The protein is shown as ribbons, whereas compound 2 and (+)-epibatidine are shown as sticks. The primary [i.e., (+) face] and complementary [i.e., (-) face] components of the extracellular domain are shown in yellow and cyan, respectively.

FIGURE S2: Different conformations of compound 2 (orange) (Class 1) at the (A) $\alpha 7/\alpha 7$, (B) $\alpha 3/\beta 4$, and (C) $\alpha 4/\beta 2$ subunit interfaces, and different conformations of (D) compound 1 (green), (E) compound 6 (Class 2) (green), and (F) compound 9 (Class 3) (green) at the $\alpha 7/\alpha 7$ subunit interface. The primary [i.e., (+) face] and complementary [i.e., (-) face] components are shown in yellow and cyan, respectively, whereas the oxygen, nitrogen, and hydrogen atoms are shown in red, blue, and white, respectively. The distance (in Å) between hydrogen bond donors and acceptors forming (full lines) and not forming (broken lines) hydrogen bond interactions are labeled. The natural mutation $\alpha 7$ -His105 to $\alpha 4/\alpha 3$ -Tyr105 and the number of hydrogen bonds are important for receptor specificity.

FIGURE S3: Molecular dynamics simulations of compound 2 at the three postulated PAM sites on the $\alpha 4\beta 2$ AChR. (A) RMSD values for compound 2 when it binds to the $\alpha 4/\beta 2$ subunit interface domain (black line), to the transmembrane domain (red line), and to the extracellular-transmembrane junction (blue line). Location of compound 2 before (blue) and after (green) 10-ns dynamics simulations when is bound to (B) the subunit interface domain, (C) the transmembrane domain, and to (D) the extracellular-transmembrane junction. The protein is shown as ribbons, whereas the compound 2 is shown as stick.

The primary [i.e., (+) face] and complementary [i.e., (-) face] components of the subunit interface are shown in yellow and cyan, respectively, whereas the transmembrane segments are shown in fuchsia. The molecular dynamics results on the h α 3 β 4 AChR are similar to that for the h α 4 β 2 AChR.

Figure S1:

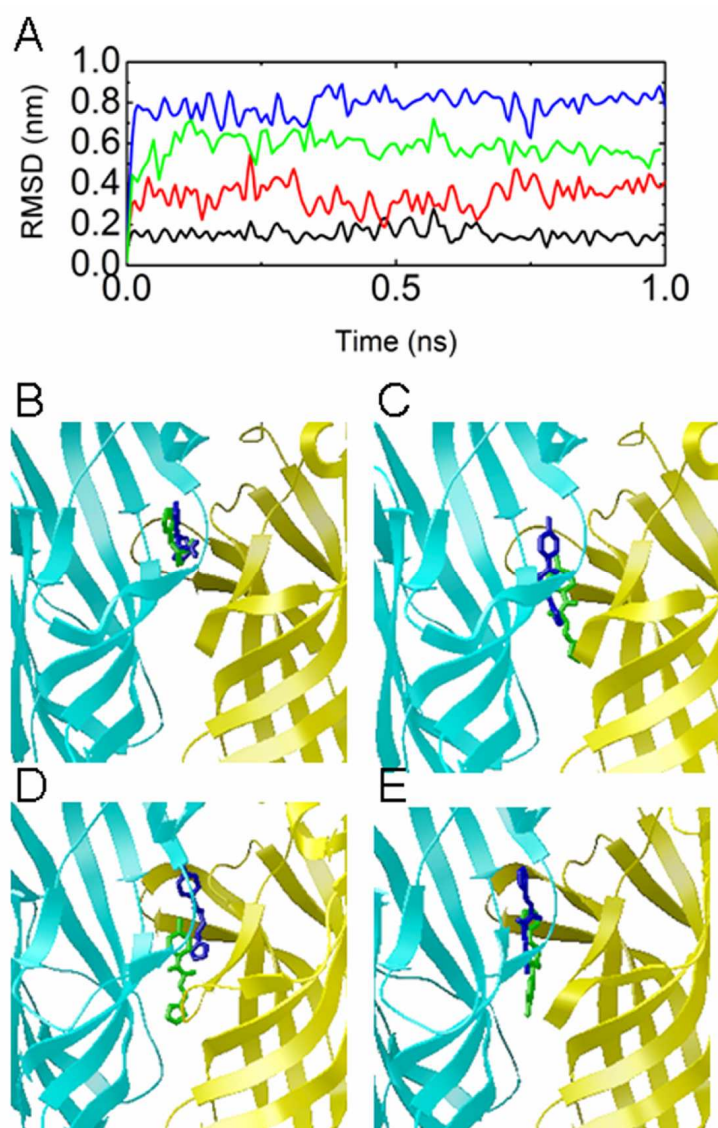


Figure S2:

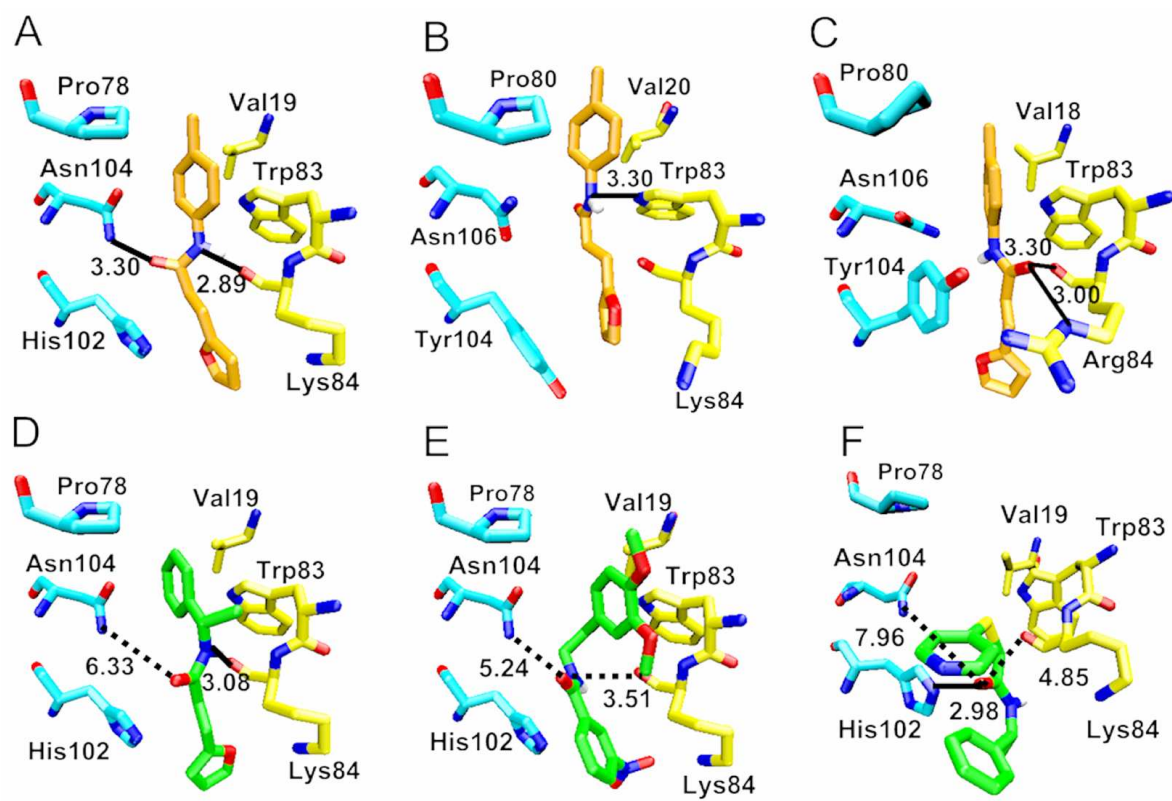


Figure S3

